JOURNAL OF CATALYSIS 26, 51–62 (1972)

Nucleation and Growth of Carbon Deposits from the Nickel Catalyzed Decomposition of Acetylene

R. T. K. BAKER, M. A. BARBER, P. S. HARRIS,
F. S. FEATES, AND R. J. WAITE

Applied Chemistry Division, Atomic Energy Research Establishment, Harwell, Didcot, Berkshire, England

Received August 23, 1971

In the presence of a nickel catalyst, acetylene decomposed to form carbonaceous solids with filamentary, amorphous, or laminar form. By observing the initiation processes continuously, parameters controlling the type of deposit have been established. Controlled atmosphere electron microscopy has shown the development of filaments behind particles of nickel (30–50 nm diameter) at relatively low temperatures (870 ± 20 K). At the same temperature, amorphous carbon nucleated around the nickel particles and spread until it covered the whole solid. In extended experiments, angular graphite laminae grew from large nickel particles (300 nm diameter) at 1300 K.

The catalytic activity of the nickel particles for filament growth ceased after approximately 15 s at 870 K, but it could be regenerated by exposure to either hydrogen at 1100 K, or oxygen at 1000 K. A significant increase in catalyst efficiency for filamentous growth was noted when particles of nickel were formed in hydrogen at 875 K prior to the introduction of acetylene. An explanation of this phenomenon and the mechanisms of the catalytic, deactivation, and regeneration processes are proposed.

Exposure of the carbonaceous deposits to oxygen demonstrated their different reactivities and suggested that filaments consisted of an easily oxidizable core with a relatively resistant skin.

INTRODUCTION

Previous investigations (*1–12*) have demonstrated that filaments can be formed by pyrolyzing hydrocarbons under widely varying conditions. Hofer *et al.* (*6*) examined by electron microscopy deposits formed on nickel in the presence of CO at 665 K, and observed that they were in the form of filaments from 0.01 to 0.2 μm in diameter. Many of these filaments appeared to be tubes, which may have been hollow or contained material less dense than the outside walls. Several workers observed or postulated that filaments grew from catalyst particles. In some cases such particles were seen at the growing end of the filament (*5–7, 9, 11*), whereas in other cases they appeared to have been left behind, apparently serving only to initiate growth of the filament (*3, 8*). In the presence of hydrocarbons, the growth of filaments catalyzed by iron, nickel, and cobalt, their oxides or carbides, generally occurs at relatively low temperatures (620–870 K), whereas temperatures in excess of 1270 K are required for growth on graphite, lampblack and silicon, where the catalyst is conceivably finely divided carbon.

The formation of highly orientated laminar graphite from the pyrolysis of hydrocarbons is well documented (*13–16*). Presland *et al.* (*15*) produced graphite platelets from the decomposition of acetylene (0.05 kN m^{-2}) on a single crystal of nickel at 1300 K. Similar graphitic laminae were observed during the catalytic decomposition of CO by single crystal nickel films (*2*).

In this paper we report the continuous observation of the processes of nucleation and growth of filamentous, amorphous, and graphitic materials from the nickel catalyzed decomposition of acetylene.

Methods

Technique

The apparatus consists of a gas reaction cell, built within a JEM 7A electron microscope, which allows specimens to be continuously exposed to a gas atmosphere at pressures up to 30 kN m^{-2} and temperatures up to 1500 K (*17*). The central area of the electron beam passes through a 20 mm hole cut in the center of the fluorescent viewing screen and strikes a transmission phosphor. The underside of the phosphor is viewed by a "Plumbicon" television camera outside the vacuum chamber. The camera output can be viewed directly on a monitor and recorded on videotape for subsequent replay and detailed analysis of the results frame by frame. Overall magnifications on the monitor screen are up to 2×10^5.

Materials

Silica films or single crystal graphite were used as supports for the specimens. The silica films were prepared by vacuum evaporation of a 50/50 mixture of SiO_2/Si on a Pyrex slide, which had been coated with a film of detergent. The resulting silica film was scored into small squares and floated on a clean water surface. The support was finally mounted over a hole in a silica coated platinum heater. Graphite crystals, obtained from Ticonderoga, New York, were cleaved by the standard procedure (*18*), heated *in vacuo* at 1175 K for 30 min to reduce surface contamination, and finally mounted on the platinum heater of the gas cell.

Spectrographically pure nickel wire (0.13 mm diameter and 3.05 mm long) was evaporated onto the support at 10.0 mN m^{-2} from a tungsten filament to produce a continuous film of nickel at least one atom thick. In other experiments sections of commercial nickel electron microscope grids were spot welded across the hole in the platinum heater ribbon.

The gases used in this work, acetylene, hydrogen, and oxygen, were all >99% pure and were used without further purification. Reaction times were between 30 to 60 min.

Results

Formation of Carbonaceous Deposits

When acetylene was pyrolyzed over nickel, three forms of carbonaceous deposit were observed; amorphous, filamentary, and graphitic.

a. Amorphous carbon. At 825 K, with both silica and graphite supports, the nickel film nucleated to form small particles (~30 nm diameter) in the presence of 0.05 KN m^{-2} acetylene. At 850 K a flocculent amorphous deposit was formed around these particles. When the pressure of acetylene was increased, the amount of flocculent deposit increased, eventually covering the whole support and obscuring many of the surface features. The nature and amount of the deposit was identical on both silica and graphite supports under similar conditions. However, with a silica film support, the deposit also formed around isolated silica particles present on the surface. In the absence of the electron beam there was a reduction in the amount of flocculent deposit.

b. Filamentary carbon. On raising the temperature to ~870 K, the nickel particles became mobile and filaments were observed to grow beneath the nickel particles, which ultimately lost contact with the support. Variation of the acetylene pressure from 0.05 to 0.26 kN m^{-2} did not result in an increase in either the number of filaments produced or their linear growth rate.

Similar filamentary growth was observed at the edges of a nickel strip when the latter was heated to 870 K in 0.05 kN m^{-2} acetylene. From continuous observations in many experiments, several features of this reaction were apparent. The diameter of the filaments was always the same as that of the nickel particles at their head. Moreover, each active nickel particle was responsible for the growth of only a single fila-

ment. This observation is to be contrasted with the iron/acetylene system, where some active iron particles were observed to disintegrate during filament growth with the result that many thinner branched filaments were also formed on the sides of the thicker parent filament (*19*). At 870 K the majority of filaments produced from nickel catalysis were about 30 nm diameter with a few exceptionally thick ones of about 100 nm diameter. The filaments grew with random paths forming loops, knots, and interconnected networks. After about 10–15 s at 870 K the nickel particles lost their mobility and the filaments ceased to grow. Figure 1A is a micrograph of a particularly thick filament and there is evidence, on the more transparent sections, of a hollow channel running the length of the filament. The more electron dense zones along the filament are where the growth has either changed direction from lateral to perpendicular or overlapped with a previously formed section. Figure 1B is a micrograph of an exceptional filament where the catalyst particle has been rotating on an axis perpendicular to the direction of filament growth.

It has been possible to obtain quantitative data on the dimensions of the filaments from frame-by-frame analysis of 16 mm ciné film. From measurements of ten particularly large diameter filaments the dimensions were:

Filament outer diameter	94–87 nm
Diameter of central core	58–56 nm (including a central hollow channel of about 10 nm)
Thickness of filament wall	18–15 nm

Experiments conducted in the absence of the electron beam produced filaments with identical characteristics to those grown in the presence of the beam at the same temperature, indicating that electron bombardment does not have any direct effect on filament formation.

Figure 2 presents data for the linear growth rate of filaments from acetylene at 0.05 kN m^{-2} under various conditions at 870 K. The sigmoid shape of the two curves (A) and (B) is typical of those usually found and is that expected for a process in which a catalyst is gradually poisoned. There did not appear to be any difference in growth rate between filaments on graphite and silica supports, or for growth on a nickel strip under the same conditions, indicating that the support plays no active chemical role in the reaction. Results in Table 1 show no correlation between filament diameter and rate of linear growth.

TABLE 1
VARIATION OF RATE OF FILAMENT GROWTH AND FILAMENT DIAMETER IN ACETYLENE AT 0.05 kN m^{-2} AND 870 K

Filament diameter (nm)	Rate of linear growth (nm s^{-1})
36	52.0
30	90.0
30	76.5
27	72.5
21	65.0
15	80.0

From measurements of over fifty filaments the filament lengths when growth ceased were between 0.53–1.1 μm, with a few exceptional filaments of up to 7 μm in length.

c. Graphite platelets. At temperatures above 1300 K in the presence of acetylene at 0.05 kN m^{-2}, a few platelets were observed to grow from the edges of some of the larger nickel particles (~300 nm diameter) which had lost their mobility. The platelets were crystalline, and interference patterns passed across them if they were induced by heating to move over the graphite support. They possessed many angular edges, the characteristic 120° angle of graphite predominating. This type of deposit was most frequently observed when the nickel was supported on a graphite single crystal. However, when there had been a heavy initial deposit of amorphous material around nickel particles supported

FIG. 1. A. Transmission electron micrograph of a carbon filament showing the internal structure of the more transparent areas (×49,500). B. Transmission electron micrograph of an exceptional filament which has formed by spiral growth (×23,250).

on a silica film and the temperature was raised to above 1300 K, similar platelet growths were observed on the metal particles.

Oxidation of Carbonaceous Deposits

When acetylene was replaced by oxygen at 1.3 kN m^{-2} and the temperature was gradually increased, the various deposits oxidized at different rates. The featureless central core of the filaments oxidized first at 970 K, leaving a more dense and relatively oxidation resistant tube. As the core material was removed, the nickel particles at the head of some of the filaments were observed to fall back down the tube leaving an open-ended structure. During oxidation, the filament wall appeared to react in spiral fashion suggesting that the tube might have the form of a scroll extending continuously along the length of the filament. The partially oxidized filaments were free of the underlying support surface and moved over it in random paths. Their motion suggested that even at this stage they still possessed a high degree of rigidity. Figure 3 is a sequence of four frames at 15 s intervals taken from 16 mm ciné film of the oxidation of a coiled filament. The coil is viewed end-on and reacted in oxygen at 0.05 kN m^{-2} and 970 K. It can be seen that there is a preferential removal of the core material and ultimately only the skin of the filament remains.

Simultaneously, the amorphous carbon deposit on the support surface oxidized, principally as a result of the migration of nickel particles which acted as oxidation

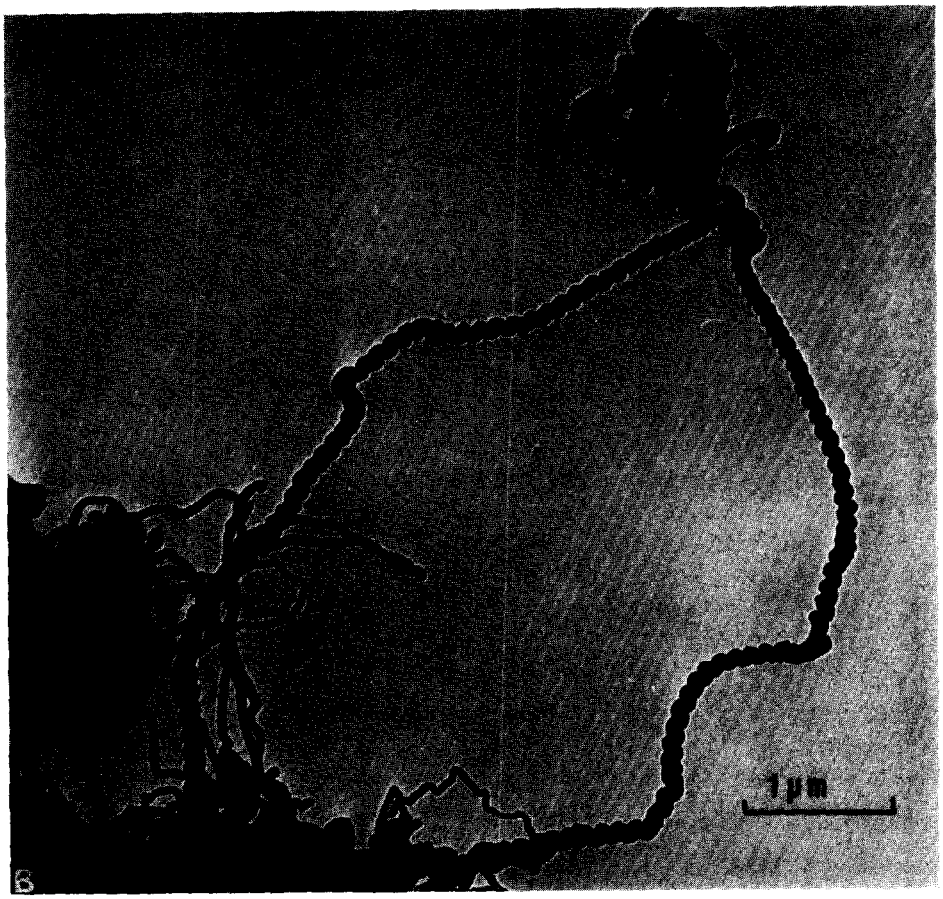

FIG. 1. (*Continued*)

catalysts, but also by uncatalyzed oxidation. The disappearance of this material, seen as the mottled grey material, is shown in the sequence in Fig. 4; the darker material remaining is nickel.

If the oxidation was continued and the temperature raised to 1100 K, oxidation catalyzed by nickel particles was observed to proceed from edges and steps on the basal plane of the supporting graphite crystal. This oxidation was characterized by the development of channels in the graphite crystal with the catalyst particle moving at the head of each channel. Most of these channels were straight, with sharp bends at angles characteristic of the underlying graphite structure. This type of behavior has been seen in independent experiments and contrasted with catalytic oxidation of the amorphous deposit, where catalyst particles moved with random paths, indicating the relative disorder of the deposit structure. At the same temperature both the skin of the filaments and the platelet material on the edges of large nickel particles underwent uncatalyzed oxidation.

Regeneration of Deactivated Catalytic Particles

In some experiments the oxidation reaction was terminated as soon as the filaments had been removed so that only the nickel particles remained on the support. When oxygen was replaced by acetylene, these previously inactive particles immediately led to further filamentary growth of carbon at 870 K.

Similar results were obtained following hydrogen treatment of the deactivated nickel particles. When filaments ceased to grow in the presence of acetylene, the hydrocarbon was replaced by hydrogen and

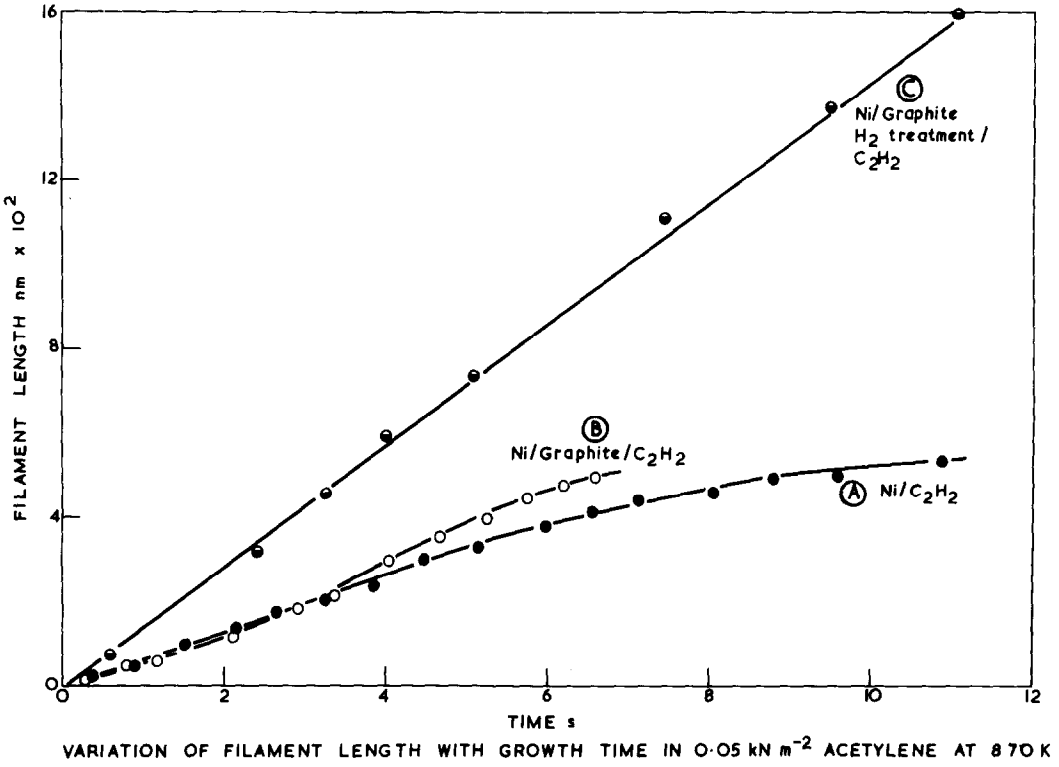

FIG. 2. Variation of filament length with growth time in acetylene at 0.05 kN m^{-2} and 870 K.

the specimen was heated at 1100 K for 5 min in the presence of hydrogen at 0.4 kN m^{-2}. No obvious changes in surface morphology were observed during this reaction, but when acetylene was reintroduced into the system existing filaments continued their interrupted growth and new filaments appeared.

Formation of Nickel Particles in Argon and Hydrogen

When the nickel film on a graphite crystal support was heated to 870 K in either argon or hydrogen at 0.05 kN m^{-2}, the nickel nucleated to form small particles (30 nm diameter) in both cases. However, subsequent exposure of these systems to acetylene at 0.05 kN m^{-2} showed differences in behavior. Nickel particles nucleated in hydrogen produced filaments of ~15.0 μm in length and grew for periods of up to 90 s when exposed to acetylene. Exposure to acetylene of particles nucleated in argon, however, behaved in a manner similar to those which were exposed directly to the hydrocarbon, producing filaments of ~1.0 μm in length and only grew for about 12 s.

Curve (C), Fig. 2 shows the growth rate from pretreatment of nickel with hydrogen and indicates a rate of 160 nm s^{-1} compared with 90 nm s^{-1} for direct exposure to acetylene. Under all conditions, however, the majority of filaments were still between 30 and 60 nm diameter.

DISCUSSION

Reaction Mechanism

Reaction mechanism of filament formation. Filaments were observed in all cases to have a metal particle at one end and part of the surface of the metal was protected towards adsorption from the gas phase by the filament. In cases where filaments had ceased to grow, the catalyst particle was seen to be encapsulated by a layer of carbon. Examination at high magnifications revealed the presence of a co-

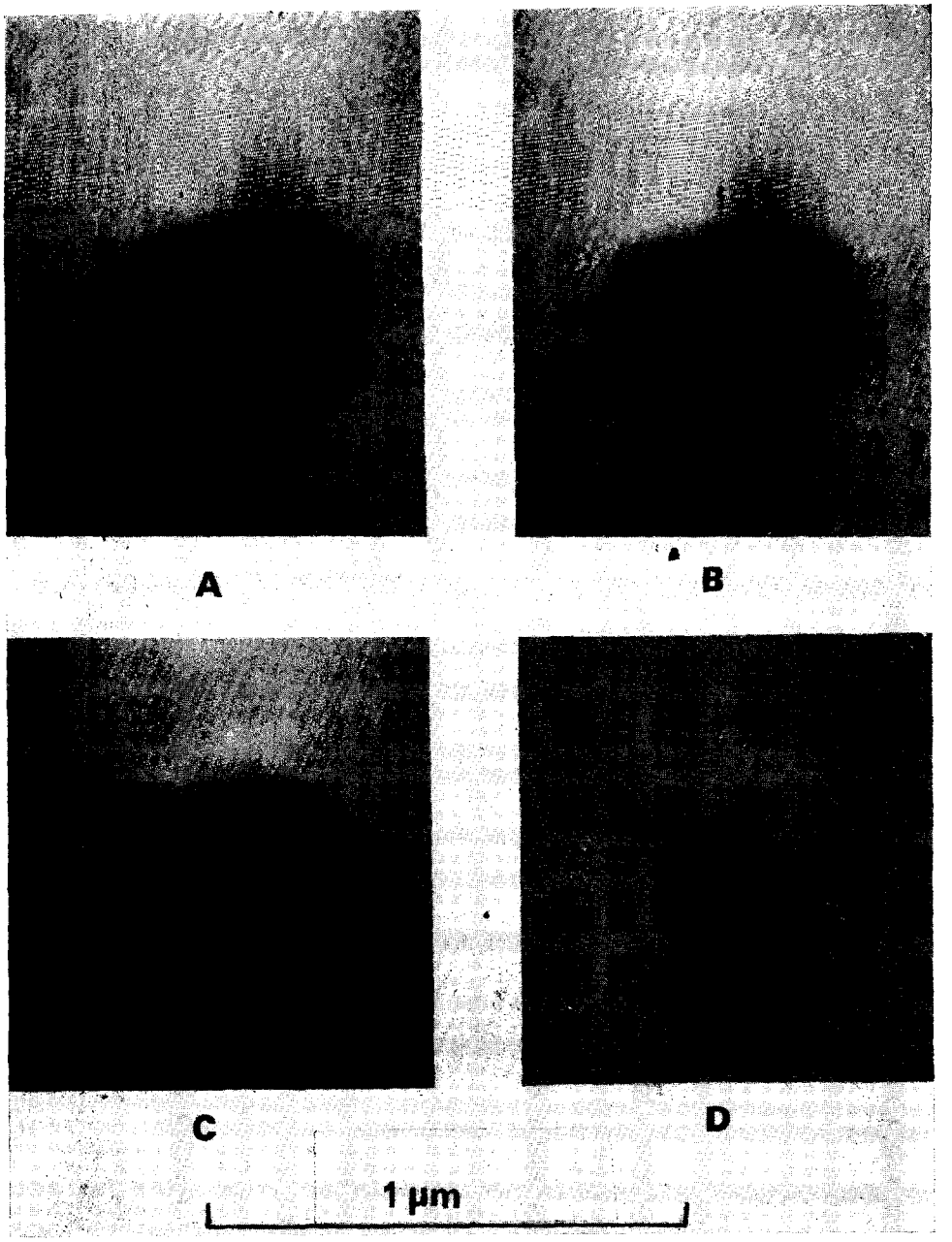

FIG. 3. Oxidation of coiled filament viewed end on in oxygen at 0.05 kN m^{-2} at 970 K (time interval between each frame is 15 s) (×72,200).

axial electron transparent channel within the filament and showed that the catalyst particle at the filament tip was "pear-shaped," with the base in the direction of growth. Oxidation experiments clearly demonstrate that the filaments have a structure with an outer sheath of relatively oxidation resistant material, probably graphitic, with a region of more readily oxidized material within it. Formation of flocculent amorphous carbon around nickel particles was observed to precede the growth of the filaments.

The curves (A) and (B) in Fig. 2 are sigmoid and three separate growth regions can be distinguished; an initial growth

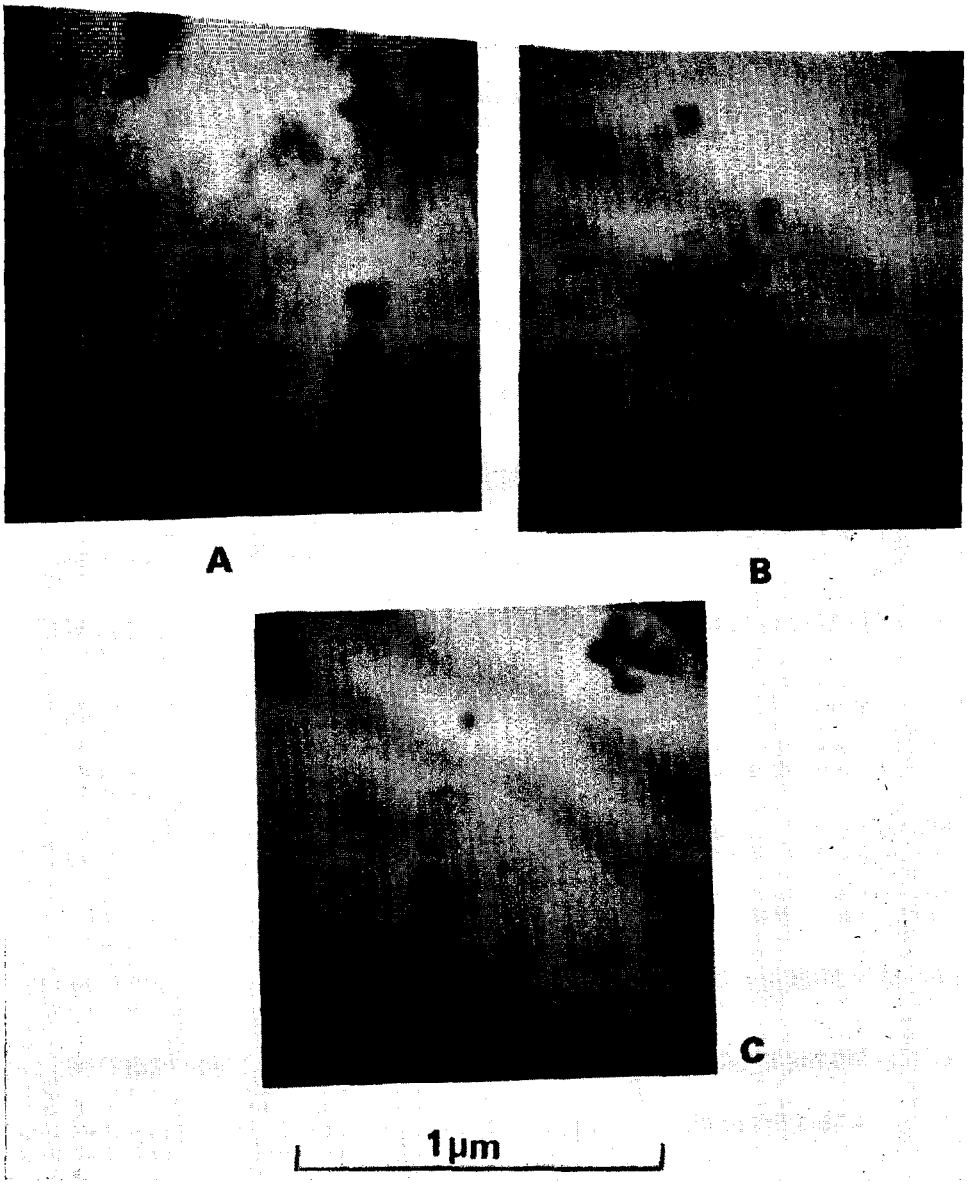

FIG. 4. Catalyzed and uncatalyzed thermal oxidation of flocculent amorphous carbon in oxygen at 1.3 kN m^{-2} and 970 K (time interval between each frame is 10 s) (×52,200).

period (zone 1), a region of constant growth rate (zone 2) and a tailing off period (zone 3). If it is assumed that the initial flocculent deposit observed is essential for subsequent filament growth on nickel, then the following mechanism adequately accounts for all the observed features. Consider the situation depicted in Fig. 5(b), acetylene decomposes on the exposed surfaces of the nickel particle and releases a considerable amount of heat, equal to $-\Delta H_f$ for $C_2H_2 + \Delta H_{soln}$ for C in Ni, the values for which are -223.6 kJ mol^{-1} (*20*) and -40.5 kJ mol^{-1} (calculated from data in ref. (*21*)), respectively. Since acetylene is unlikely to decompose so rapidly on protected regions of the particle a temperature gradient will be set up within the particle, which is steepest in the regions immediately adjacent to those covered by the

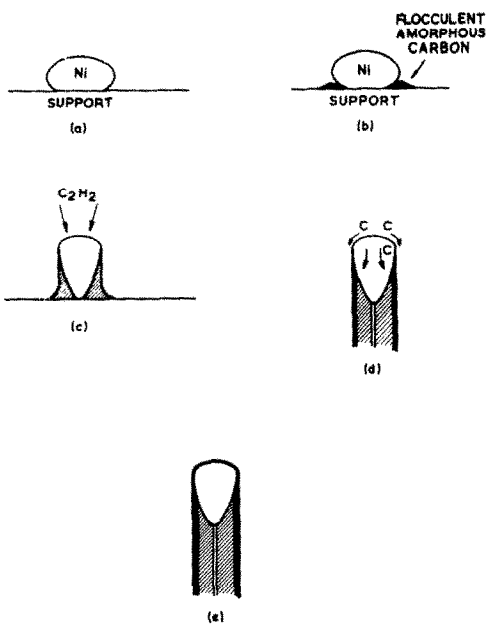

FIG. 5. Stages in the growth of filaments.

flocculent deposit. Carbon from decomposed acetylene is taken into solution, diffuses down the thermal gradient to be deposited predominantly in the protected regions to produce the situation shown in Fig. 5(c). The precipitation of carbon at the rear of the particle builds up a deposit of carbon which forces the particle away from the support. This initial mode of growth is responsible for the distortion of the particle as shown in Figs. 5(b) and 5(c). For such distortion to occur the metal must be assumed to have properties of a liquid, which is reasonable (*22*, *23*). In that event, the ultimate detachment of the particle from the support will be so rapid that deposition of carbon in this region will probably not have taken place, which accounts for the initial appearance of a hollow channel. This could explain the initiation period.

The increasing growth rate in zone 1 (Fig. 2) is a result of an increase in the mean temperature of the particle, due to the fact that the particle is no longer in contact with a heat sink (the filament acts as an insulator). The rate of carbon transport through the particle increases and consequently the filament growth rate increases. If diffusion of carbon through the particle is the rate determining step, then excess carbon from the decomposition of acetylene will be deposited at the exposed face of the particle. The difference in character between the skin and bulk materials of the filaments is quite definite and suggests that these two phases are produced by different processes. It is possible that the bulk material arises from carbon transported through the particle and the skin by carbon transport around its peripheral surfaces, as shown in Fig. 5(d). Carbon deposited at the rear of the particle loses contact with the metal in a shorter time after its formation than that constituting the skin. It would thus be expected that the bulk material of the filament would show less structural order than the skin and as a consequence a higher reactivity towards oxygen. Deposition of carbon at the rear face of the particle is an endothermic reaction ($+40.5$ kJ mol^{-1}): therefore the regions where precipitation takes place to the greatest extent will be at lowest temperature.

Zone 2 growth at constant rate ensues when the mean temperature of the particle reaches a maximum as the heat input from the decomposition of acetylene is balanced by losses due to radiation, conduction, etc. We have calculated that for a linear filament growth rate of 90 nm s^{-1}, and assuming a filament density of 2.2 g cm^{-3}, radiation losses balance the heat input at 900 K. The postulate that diffusion of carbon through the liquid particle determines the growth rate in zones 1 and 2 is supported by our calculations from the data of Tesner *et al.* (*4*), which yields an activation energy of 145.0 kJ mol^{-1}. This value is to be compared with values for the activation energy of the diffusion of carbon in nickel containing 0.5% carbon which lie in the range 138 to 145.5 kJ mol^{-1} (*24*).

If excess carbon on the surface does not move away to form the filament skin rapidly enough, then the fraction of free particle surface available for adsorption and decomposition of acetylene slowly decreases. Since this results in a decrease in heat input to the particle, which allows cooling and a subsequent decrease in the

rate of diffusion of carbon through the particle, a consequent slowing of the growth rate is observed. Ultimately, the situation shown in Fig. 5(e) is reached, where the particle is completely encapsulated by surface carbon and filament growth ceases as observed on particles which had lost their activity.

It was observed that when the filaments were combusted in oxygen so that all the carbon was removed, filamentous growth proceeded when acetylene was reintroduced, and the growth rate curves are similar in form and magnitude. This is consistent with the removal by oxidation of the carbon covering the particle, a process which would be catalyzed by the nickel surface itself. There is the possibility that nickel could have contained an appreciable amount of oxygen after such treatment. Since the growth characteristics of these oxygen-containing particles were similar to those of the original particles, one may conclude that either the original particles also contained oxygen or that the oxygen-containing particles were reduced to the metal during the filament growth process. The initial presence of appreciable amounts of oxygen in the original nickel particles would tend to delay the attainment of maximum growth rate. A fraction of the dissolved carbon would be lost by reaction with oxygen resulting in a slower rate of growth than if all the dissolved carbon precipitated to form the filament. As the rate of carbon diffusion in the particle is not a maximum, the accumulation of carbon on the exposed face is more rapid than if the particle had not contained oxygen. This being the case it is possible that zones 1 and 3 (Fig. 2 curves (A) and (B)) overlap to give only a point of inflection rather than distinct zone 2 growth. The apparent maximum growth rate is expected to be always lower than the real value obtained from oxygen free particles.

Nucleation of the nickel film in hydrogen followed by reaction with acetylene produced filaments which grew longer and at a faster rate (Fig. 2 curve (C)). Hydrogen would be expected to remove all oxygen from the particle and as a consequence the maximum temperature gradient would be attained in a shorter time accounting for the observed effects.

Amorphous Deposit Formation

The support material does not appear to influence the formation of amorphous deposit around small nickel particles; similar material was formed on graphite and silica supports. It is probable that this deposit arose from gas phase polymerization of acetylene, and that the nickel particles merely acted as nucleating centers for its physical accumulation on the surface. This deduction is substantiated by the fact that silica particles were also effective in their action as nuclei for deposit aggregation. However, Johnson and Anderson (*25*) studied the vapor phase production of carbon by pyrolysis of acetylene at 825–1300 K and found that polymer droplets, formed at 975 K, remained quite stable; also at this temperature the first solid reaction products were observed.

Since the absence of the electron beam reduced the amount of amorphous deposit formed, radiation processes may be involved to some extent in its formation. It has been shown that the radiolysis of acetylene produces a high molecular weight polymer (*26*), probably cuprene, and benzene (*27*) and it is possible that the latter may be an important intermediate in the production of carbon. Field (*28*) irradiated acetylene with 2 MeV electrons and observed both benzene and polymer formation. The reaction mechanism whereby benzene and the polymer are formed is not established. The polymer is probably formed by a chain reaction, but the chain carriers may be ions, free radicals or both. Benzene is generally assumed to be formed from neutral species (*29*).

Graphite Platelet Formation

The growth of graphite plates by pyrolysis of various carbon-containing gases over nickel is well documented (*2, 13–15*).

Grenga and Lawless (*2*) stated that graphite platelets formed on the (111) surfaces of the metal after only a few minutes reaction with CO at 825 K. The (110) surface was the least active and graphite deposition occurred only after several hours of treatment. Walker *et al.* (*14, 15*) showed that deposition of laminar graphite by the pyrolysis of acetylene at 1300 K over nickel only occurred when the nickel surface was substantially free of oxide. They concluded that the graphite laminae grew most effectively on the (110) surface by an epitaxial process. Karu and Beer (*13*) produced thin crystalline films of graphite from the pyrolysis of methane over nickel foils at 1175–1375 K.

It is doubtful whether the graphite platelets observed in the present study are formed by an epitaxial process as they grew almost exclusively on nickel particles supported on a graphite support. Platelet formation occurred on only isolated nickel particles (300 nm diameter) and appeared to coincide with loss of mobility of these particles. It therefore seems reasonable to suppose that the platelets are formed by surface diffusion involving carbon transport from either the graphite support or the amorphous deposit to catalytically active sites near nickel particles. Nickel dissolves 0.23 wt % of carbon at 1300 K (*21*), and it is possible that the metal loses its mobility when the amount of dissolved carbon approaches this value. The gas stream would provide a temperature gradient through the particle allowing graphite to crystallize on the edges of the nickel (*30*). The failure to observe platelet formation on a significant scale with a silica support is probably due to the lower relative rate of solubility of carbon from the amorphous deposit compared to that from graphite (*31*).

Acknowledgments

The authors are indebted to Mr. J. Wright and Mr. R. B. Thomas (Applied Chemistry Division, AERE Harwell) and Dr. D. L. Trimm (Imperial College, London) for helpful discussions.

References

1. Iley, R., and Riley, H. L., *J. Chem. Soc.* 1362 (1948).
2. Grenga, H. E., and Lawless, K. R., *Electron Microsc., 6th Proc. Int. Congr. Kyoto* 551 (1966).
3. Tesner, P. A., and Echeistova, A. I., *Dokl. Akad. Nauk USSR 87,* 1029 (1952).
4. Tesner, P. A., Robinovich, E. Y., Rafalkes, I. S., and Arefieva, E. F., *Carbon* **8,** 435 (1970).
5. Davis, W. R., Slawson, R. J., and Rigby, G. R., *Nature* **171,** 756 (1953).
6. Hofer, L. J. E., Sterling, E., and McCartney, J. T., *J. Phys. Chem.* **59,** 1153 (1955).
7. Davis, W. R., Slawson, R. J., and Rigby, G. R., *Trans. Brit. Cer. Soc.* **56,** 67 (1957).
8. Meyer, L., *Z. Krist.* **109,** 61 (1957).
9. Walker, P. L., Jr., Rakszawski, J. F., and Imperial, G. R., *J. Phys. Chem.* **63,** 133, 140 (1959).
10. Bacon, R., *J. Appl. Phys.* **31,** 283 (1960).
11. Renshaw, G. D., Roscoe, C., and Walker, P. L., Jr., *J. Catal.* **18,** 164 (1970).
12. Ruston, W. R., Warzee, M., Hennaut, J., and Waty, J., *Carbon* **7,** 47 (1969).
13. Karu, A. E., and Beer, M., *J. Appl. Phys.* **37,** 2179 (1966).
14. Presland, A. E. B., and Walker, P. L., Jr., *Carbon,* **7,** 1 (1969).
15. Presland, A. E. B., Roscoe, C., and Walker, P. L., Jr., *Ind. Carbon Graphite Conf. (London),* 1970.
16. Blau, G., and Presland, A. E. B., *Ind. Carbon Graphite Conf. (London),* 1970.
17. Feates, F. S., *Chem. Ind.* 1103 (1970).
18. Hennig, G. R., "Chemistry and Physics of Carbon" (P. L. Walker, Jr., ed.), Vol. 2. Dekker, New York, 1966.
19. Baker, R. T. K., and Thomas, R. B., unpublished.
20. Stull, D. R., Westrum, E. F., Jr., and Sinke, G. C., "The Chemical Thermodynamics of Organic Compounds," p. 334. Wiley, New York, 1969.
21. Hansen, M., "Constitution of Binary Alloys," 1958; Elliott, R. P., Suppl. 1, 1965; Shunk, F. A., Suppl. 2, 1969; McGraw-Hill, New York.
22. Chopra, K. L., "Thin Film Phenomena," McGraw-Hill, New York, 1969.
23. Behrndt, K. H., *J. Appl. Phys.* **37,** 3841 (1966).
24. Diamond, S., and Wert, C., *Trans. Met. Soc. AIME* **239** (5), 705 (1967). Shavensin,

A. B., MINKEVITCH, A. H., AND SCHERBINSKI, C. B., *Izv. Vyssh. Ucheb. Zaved. Chern. Met.* **1**, 95 (1965). GRUZIN, P. L., POLICKARPOV, YU. A., AND FEDEROV, G. B., *Fiz. Metal. Metalloved.* **4** (1), 94 (1957).

25. JOHNSON, G. L., AND ANDERSON, R. C., *Conf. Carbon, Proc. 5th* **1**, 395 (1961).

26. LIND, S. C., BARDWELL, D. C., AND PERRY, J. H., *J. Amer. Chem. Soc.* **48**, 1556 (1926).

27. MUND, W., AND ROSENBLUM, C., *J. Phys. Chem.* **41**, 469 (1937).

28. FIELD, F. H., *J. Phys. Chem.* **68**, 1039 (1964).

29. FREEMAN, G. R., *Rad. Res. Rev.* **1**, 1 (1968).

30. KURNAKOW, N. S., AND ZEMCZUZNY, S. F., *Z. Anorg. Chem.* **54**, 149 (1907).

31. RILEY, R. V., 48th Annual Meeting Inst. British Foundrymen (Newcastle), Paper 997 (1951).